MALAYSIAN JOURNAL OF ANALYTICAL SCIENCES

Journal homepage: https://mjas.analis.com.my/

Research Article

A novel of substituted dithiocarbazate derivatives: synthesis, characterisation, and antibacterial activity of *S*-benzyl-β-*N*-4-chloro-3-nitrobenzoyl dithiocarbazate (SB3NO) and its Cu(II), Zn(II), Co(II), and Ni(II) complexes

Siti Khadijah Roslan, and How N.-F Fiona*

Department of Chemistry, Kulliyyah of Science, International Islamic University Malaysia (IIUM), 25200, Kuantan, Pahang, Malaysia

*Corresponding author: howfiona@iium.edu.my

Received: 11 December 2024; Revised: 15 April 2024; Accepted: 28 April 2025; Published: 15 June 2025

Abstract

Cu(II), Zn(II), Co(II), and Ni(II) metal complexes have been synthesized using the *O, S* bidentate ligand *S*-benzyl-4-chloro-3-nitrodithiocarbazate (SB3NO). SB3NO coordinates with the metal ions according to the general formula of $[M(SB3NO)_2]$, where M is Cu^{2+}, Zn^{2+}, $Co^{2+,}$ and Ni^{2+}. Various spectroscopic techniques, such as elemental analysis, FT-IR, NMR, GC-MS, TGA, UV-Vis spectroscopy, molar conductivity measurements, and magnetic susceptibility testing, were used to characterize the ligand and complexes. In a solid state, SB3NO exists in a thione tautomeric form and deprotonated to chelate metal(II) center through the oxygen of carbonyl and ionic sulfur of thiol in liquid, giving rise to either tetrahedral or square planar geometry. Additionally, the *in-vitro* antibacterial activity of SB3NO and its metal complexes was assessed against pathogenic gram positive and gram-negative bacteria. The test revealed that $Zn(SB3NO)_2$ exhibited the strongest antibacterial activity against *Pseudomonas aeruginosa* (ATCC 27853) in the MIC assay (437 µg/ml). This study concludes that incorporating metal ions enhances the antibacterial activity of the free ligand, highlighting their potential as promising metal-based antibacterial agents.

Keywords: Dithiocarbazate derivatives, metal complexes, MIC assay

Introduction

The rise of multidrug-resistant (MDR) bacterial strains has created an urgent need for new and more effective antimicrobial agents. Many conventional antibiotics have become ineffective due to bacterial resistance mechanisms, highlighting the urgency of developing alternative therapeutic strategies. Metal-based antibacterial agents offer a promising solution, as their distinct mechanisms of action differ from those of traditional organic antibiotics [1]. Metal ions can interact with biomolecules, induce oxidative stress, and disrupt essential bacterial processes, making them potential candidates for antimicrobial applications [2,3]. Transition metal complexes, particularly those incorporating copper (Cu), zinc (Zn), cobalt (Co), and nickel (Ni), have demonstrated significant antibacterial properties [4]. Their coordination with bioactive ligands enhances stability, solubility, and biological activity, resulting in improved antibacterial efficacy [5].

Among the various classes of metal-based antibacterial agents, dithiocarbazate derivatives have garnered significant attention due to their strong chelating properties and bioactive potential [6,7]. These compounds, characterized by nitrogen and sulphur donor atoms, readily coordinate with transition metals to form stable metal complexes. Previous studies have shown that metal complexes derived from dithiocarbazate derivatives possess strong antibacterial, antifungal, and anticancer properties. Moreover, research has demonstrated that the metal complexes from dithiocarbazate derivatives frequently exhibit superior antibacterial activity compared to their free ligands [8], [9], making them an attractive avenue for drug development. However, despite their promising biological applications, further structural modifications and optimizations are necessary to enhance their efficacy, selectivity, and pharmacokinetic properties.

Hence, this study aims to contribute to the growing field of metal-based antibacterial agents by synthesising and characterising a new ligand and its metal complexes, while providing insights into their structure-activity relationships. Specifically, we report the synthesis, characterization, and biological evaluation of a novel substituted dithiocarbazate derivative, *S*-benzyl-β-*N*-4-chloro-3-nitrobenzoyl dithiocarbazate (SB3NO), along with its Cu(II), Zn(II), Co(II), and Ni(II) metal complexes. This work focuses on the development of a newly designed dithiocarbazate derivative incorporating electron-withdrawing functional groups (Cl and NO_2) within the ligand framework, which has not been previously explored for its antibacterial properties. The presence of these functional groups is expected to enhance the ligand's coordination ability and biological activity. Furthermore, the formation of its transition metal complexes introduces structural modifications that may improve antibacterial potency through enhanced metal-ligand interactions.

Materials and Methods

Instrumentation

Melting points were determined using an Electrothermal™ IA9300 apparatus. Infrared Spectroscopy (IR) was recorded in the range of 400-4000 cm^{-1} using KBr pellets on a Perkin Elmer 96255 Fourier Transform Infrared Spectroscopy (FTIR) spectrometer. The molar conductance of each metal complex was measured in a 10^{-3} M solution of Dimethyl Sulfoxide (DMSO) using an Eutech CON 700 conductivity meter. Ultraviolet-Visible Spectroscopy (UV–VIS) spectra were recorded on a Shimadzu UV-1900 Series PC spectrophotometer (800-200 nm) in DMSO solution. ^{1}H Nuclear Magnetic Resonance (NMR) and ^{13}C NMR spectra were recorded on a Bruker Ultra Shield Plus 500 MHz spectrometer, using deuterated DMSO as the solvent, with tetramethylsilane (TMS) as an internal standard. Mass spectrometry was performed using a Perkin Elmer CLARUS 680 GC / CLARUS 5S8T MS. Thermogravimetric analysis (TGA) was measured using the Thermogravimetric Analyzer Shimadzu TGA-50 Series. The nitrogen gas flow rate was 10 ml/min with a heating rate of 10 °C/min. The starting temperature was 25 °C, with the maximum temperature set at 500 °C and 800 °C for SB3NO and metal complexes, respectively. Magnetic susceptibility was measured with a Sherwood Scientific MSB AUTO at 298 K. All analyses were conducted at the Physical Science Building, Kulliyyah of Science, International Islamic University Malaysia (IIUM) Kuantan Campus, except for the NMR analyses and magnetic susceptibility measurements, which were performed at the Central Laboratory, Universiti Malaysia Pahang Al-Sultan Abdullah (UMPSA) Gambang Campus and Universiti Malaya, respectively.

Preparation of *S*-benzyl dithiocarbazate (SBDTC)

SBDTC was synthesized as previously described [10] Potassium hydroxide (KOH) (0.1 mol, 5.7 g) was dissolved in 35 mL of cold 90% ethanol. This solution was then mixed with hydrazine hydrate (0.1 mol, 5 mL). The mixture was cooled in an ice salt bath until the temperature reached 0 °C. Gradually, carbon disulfide (0.1 mol, 6 mL) was added to the cooled solution with continuous stirring. Upon the addition of carbon disulfide, two layers formed. The brown oil (lower layer) was then separated and dissolved in 30 mL of cold 40% ethanol. Subsequently, benzyl chloride (0.1 mol, 11.37 mL) was added dropwise to this solution with vigorous stirring and maintaining the temperature at 0-5 °C. A white precipitate formed, which was then filtered and dried overnight over silica gel.

Preparation of *S*-benzyl-4-chloro-3-nitrobenzoyl dithiocarbazate (SB3NO)

SB3NO was synthesized following the procedure outlined [11]. Potassium hydroxide (0.01 mol, 1.983 g) was added to a solution of SBDTC (0.01 mol, 0.56 g) dissolved in 30 ml of absolute ethanol. To this solution, 4-chloro-3-nitrobenzyl chloride (0.01 mol, 1.42 mL) was added before it was stirred and refluxed for 8 hours. The solution was left standing overnight after reflux. The product obtained was filtered and dried over silica gel. The product was later recrystallized from ethanol.

Preparation of the metal complexes

The synthesis of metal complexes was carried out based on the method reported by [12]. SB3NO (0.9 nmol, 0.3 g) was dissolved in 30 mL of boiling absolute ethanol, and potassium hydroxide (0.9 nmol, 0.08 g) was added to the resultant solution. Subsequently, a hot solution of the metal salt (0.45 nmol) dissolved in 30 mL of absolute ethanol was added to the previous solution. The solution was heated and stirred for approximately 20 minutes until its volume was reduced to half. The precipitate was filtered while the solution was still hot and left to dry overnight on silica gel. The metal salts used were copper(II) acetate monohydrate (0.09 g), nickel(II) acetate tetrahydrate (0.11 g), zinc(II) acetate dihydrate (0.098 g), and cobalt(II) acetate tetrahydrate (0.11 g).

Bacteria culture

Antimicrobial activity was assessed at the Microbiology Laboratory located at the Physical Science Building, Kulliyyah of Science, IIUM Kuantan Campus. Four pathogenic bacteria were cultured following the procedures detailed in the literature [13]. The strains used were *Staphylococcus*

aureus (ATCC 25923), *Bacillus cereus* (ATCC 11778), *Escherichia coli* (ATCC 25922), and *Pseudomonas aeruginosa* (ATCC 27853). All strains were stored at -80°C and streaked on nutrient agar plates. The bacterial strains were then cultivated in nutrient broth at 37°C for 24 hours. The bacterial inocula was prepared by selecting 3-4 colonies from the agar plates and suspending them in nutrient broth, with the suspension adjusted to the 0.5 McFarland standard. The turbidity of the bacterial suspension was measured by determining the optical density (OD) at 625 nm, with an OD of 0.1 corresponding to 1.5 x 10^8 CFU/mL.

Antimicrobial assay

The antimicrobial assay was conducted to determine the Minimum inhibitory concentration (MIC, µg/mL) of the synthesized compounds, following the procedure outlined in the past literature [14]. The concentrations of the synthesized compounds and the positive controls (gentamycin and ampicillin) were prepared using two-fold serial dilutions. A stock solution of the compounds was prepared at 7000 µg/mL in 5% DMSO. 100 µL of nutrient broth was added to each microplate well, except for the first well. Then, 200 µL of the synthesized compound or positive control was added to the first well. Serial dilutions were performed and 100 µL of the bacterial suspension was added to all wells. The plates were incubated at 37°C for 24 hours. The MIC values of the compounds that exhibited no growth of microorganisms were recorded.

Results and Discussion

Synthesis, physical and analytical data

S-benzyl-4-chloro-3-nitrobenzoyl dithiocarbazate (SB3NO) was obtained through the reaction between *S*-benzyldithiocarbazate (SBDTC) and 4-chloro-3-nitrobenzyl chloride in the presence of potassium hydroxide (KOH). During the reaction, SBDTC undergoes deprotonation by KOH, increasing the nucleophilicity of SBDTC [15]. SBDTC acquires a negative charge and then facilitates the attachment of the 4-chloro-3-nitrobenzoyl group to the β-nitrogen, resulting in the formation of SB3NO (**Figure 1**). Other possible reactions could lead to Schiff base formation due to the presence of the nitro (NO_2) group at 4-chloro-3-nitrobenzyl chloride. However, due to the presence of KOH and chloride group as a deprotonating agent and leaving group, respectively, the reactions favor the nucleophilic substitution mechanism, as depicted in **Figure 1**.

In the formation of metal complexes, SB3NO undergoes tautomerisation to a thiol form in solution, with the thiol proton being deprotonated in the presence of KOH, generating thiolate anions (**Figure 2**) [16]. This process enhances the nucleophilicity of SB3NO, enabling it to act as a uninegative chelator with metal ions. Initial attempts to synthesise metal complexes from SB3NO without KOH yielded no products. However, the subsequent addition of KOH to the SB3NO mixture, prior to metal ion introduction, successfully produced the desired metal complexes.

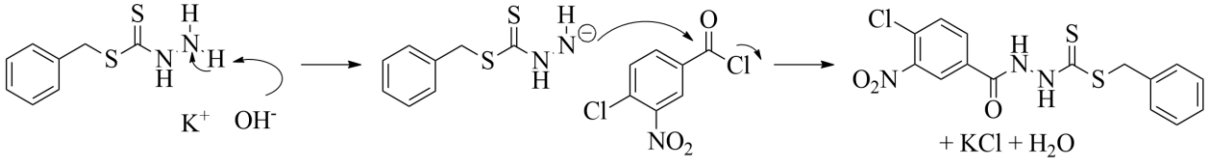

Figure 1. Mechanism reaction of SB3NO

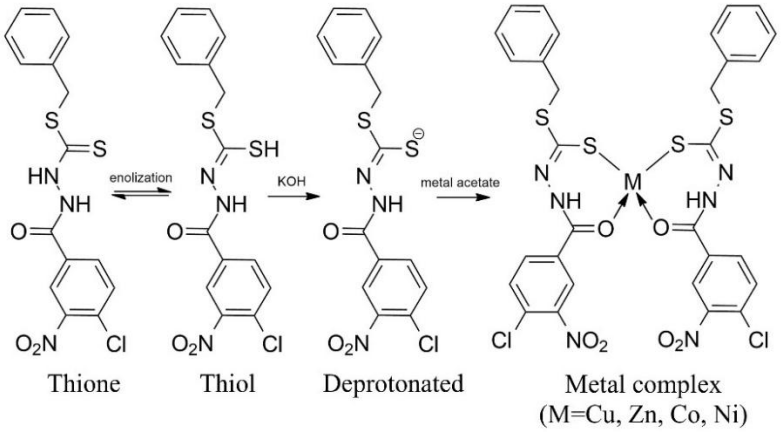

Figure 2. Mechanism reaction of metal complexes from SB3NO

The physical and analytical data for SB3NO and its metal complexes are presented in **Table 1**. The elemental analyses of the compounds were consistent with the expected values, confirming the compositions of the synthesized compounds. Despite the metal complexes being synthesised with a 1:1 ratio of metal to ligand, the elemental analyses of the metal complexes revealed a consistent metal-to-ligand ratio of 1:2 for all metal complexes. The melting point of SB3NO was in the range of 188-190 °C, while the metal complexes decomposed in the range of 256-346 °C. Furthermore, the compounds were devoid of contaminants, as evidenced by the sharp melting points. Overall, all compounds generally yielded moderate to good yields.

Infrared spectroscopy spectra

The selected adsorption bands of SB3NO and its metal complexes are listed in **Table 2**, along with their respective assignments. A weak band at 3094 cm^{-1}, attributed to the stretching vibration υ(N–H), was visible in the spectrum of SB3NO. The absence of both the asymmetric ν(N-H) and symmetric ν(N-H) of the NH_2 group found around 3304 and 3238 cm^{-1}, respectively, indicates that the 4-chloro-3-nitrobenzoyl substituent is attached on the β-nitrogen of SBDTC.

SBDTC was found to be able to undergo thione-thiol tautomerism [17]. However, SB3NO can undergo thione-thiol-thionol-thiolol tautomerism to achieve stability, as depicted in **Figure 3**. The IR data suggests that SB3NO exists solely as the thione tautomeric form in solid, as indicated by the presence of strong stretching vibration υ(C=S) and υ(C=O) at 1107 cm^{-1} and 1685 cm^{-1}, respectively. Plus, the absence of the stretching vibration of υ(S–H), typically observed between 2603-2707 cm^{-1}, rules out the presence of the thiol tautomeric form. Furthermore, the absence of the broad band around 3300 cm^{-1}, corresponding to υ(O-H), confirms that SB3NO does not exist as either the thionol or thiolol forms in the solid state.

The FTIR of the metal complexes displayed a peak attributed to the primary stretching vibration υ(N-H) around 3079-3084 cm^{-1}, indicating that there was no coordination through the proton of the amino group. Additionally, the stretching vibration band υ(N–N) was retained at approximately 1345 cm^{-1} in the metal complexes, further confirming the non-involvement of the amino group in metal complexes.

Table 1. Physical and analytical data of SB3NO and its metal complexes

Compound	Colour	M.p (ºC)	Found (Calculated %)				Metal (%)	Yield (%)
			C	H	N	S		
SB3NO	Cream	188-190	46.56 (47.18)	2.97 (3.17)	10.65 (11.00)	15.04 (16.79)	-	84
$Cu(SB3NO)_2$	Green	318	42.48 (43.56)	2.80 (2.92)	11.18 (10.16)	14.35 (15.50)	7.73 (7.68)	60
$Zn(SB3NO)_2$	Black	346	42.73 (43.46)	3.23 (2.92)	10.27 (10.14)	14.53 (15.47)	7.57 (7.89)	54
$Co(SB3NO)_2$	Brown	310	44.76 (43.80)	2.82 (2.94)	10.53 (10.22)	14.55 (15.59)	-	66
$Ni(SB3NO)_2$	Yellow	256	44.05 (43.81)	2.94 (2.94)	9.87 (10.22)	14.36 (15.59)	7.12 (7.14)	75

Table 2. Selected IR bands of SBDTC, SB3NO, and its metal complexes

Compound	IR Bands (cm^{-1})							
	***υ*(N–H)**	***υ*(C=S)**	***υ*(S-C-S)**	***υ*(C=O)**	***υ*(N–N)**	***υ*(C=N)**	***υ*(N-O₂)**	***υ*(M–S)**
SBDTC	3304, 3238, 3180	1048	952	-	1347	-	-	-
SB3NO	3094	1107	1037	1685	1353	-	1382	-
$Cu(SB3NO)_2$	3080	-	1123, 1049	1623	1345	1602	1385	485
$Zn(SB3NO)_2$	3083	-	1123, 1049	1628	1350	1597	1387	485
$Co(SB3NO)_2$	3079	-	1123, 1049	1630	1345	1600	1386	485
$Ni(SB3NO)_2$	3084	-	1123, 1043	1630	1349	1600	1385	481

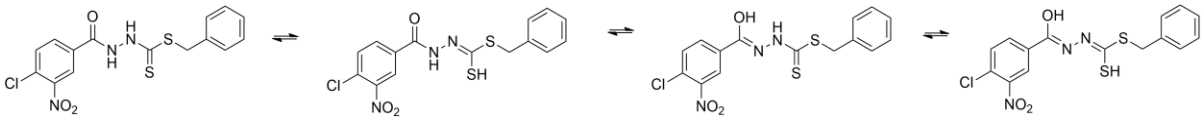

(a) Thione (b) Thiol (c) Thionol (d) Thiolol

Figure 3. The possible tautomerism of SB3NO

However, it was observed that metal complexes showed a notable negative shift of approximately 60 cm^{-1} in the stretching vibration υ(C=O) compared to the spectrum of SB3NO. This shift strongly suggests coordination between the carbonyl oxygen and the metal ion. Additionally, the absence of υ(C-O) peaks in the 1200–1300 cm^{-1} region further support coordination occurring through the C=O group. Furthermore, the stretching vibration peaks for υ(N-O_2) remained unchanged across all metal complexes, indicating that the nitro group does not participate in metal binding.

Moreover, the disappearance of υ(C=S) in the metal complexes suggests the involvement of sulphur in the formation of complexes. This is further supported by the splitting of the stretching vibration υ(S-C-S) in the range of 1043-1123 cm^{-1}, and the appearance of υ(M–S) around 481-485 cm^{-1}. Additionally, the presence of the υ(C=N) stretching vibration around 1597-1602 cm^{-1} in all the metal complex spectra confirms that they are no longer present in their thione form but rather appear to be in a thiol state. Overall, FTIR confirmed that SB3NO acts as a uninegative bidentate O, S donor, coordinating through the carbonyl oxygen and the thiolate sulfur, as illustrated in **Figure 2**.

Nuclear magnetic resonance spectra

The ^{1}H and ^{13}C NMR data of SB3NO are reported in **Table 3** and illustrated in **Figure 4**. The ^{1}H NMR spectrum suggests that SB3NO exists as thione-thiol tautomers in an equilibrium. The thione tautomeric form was indicated by two sets of doublet peaks at δ_H = 4.37, 4.39 ppm, and 4.49, 4.51 ppm, corresponding to the two neighbouring protons of the amino groups. Based on the integration of these doublet peaks, the thione-thiol tautomeric forms were found to be present in a 2:1 ratio. The thiol form is confirmed by the appearance of a singlet peak for the S–H group at δ_H = 4.59 ppm. Furthermore, the absence of peaks at approximately δ_H = 10-13 ppm corresponding to the O–H group showed that SB3NO exists neither as the thionol nor the thiolol form. Additionally, the methylene (-CH_2) group was observed as a singlet peak at δ_H = 4.59 ppm, while the aromatic protons of SB3NO were found to be present in the aromatic region, ranging from δ_H = 8.45-7.22 ppm.

The ^{13}C NMR spectrum further supports that SB3NO exists as the thione and thiol tautomeric forms. The thione form was indicated by the presence of the signals, C=S and C=O at around δ = 200.17 and 165.81 ppm, respectively. Meanwhile, the thiol form was indicated by the presence of the C=N signal at δ = 154.66 ppm. Furthermore, the methylene (CH_2) carbons for both the thione and thiol tautomeric forms were found at δ = 36.99 and 37.53 ppm, respectively. Lastly, the chemical shifts in the region of δ = 126.37 - 147.67 ppm were attributed to the carbons of the aromatic rings. Thus, based on the NMR analysis, SB3NO exists as a mixture of thione-thiol tautomers with a ratio of 2:1 in the liquid, predominantly favouring the thione form.

Mass spectrometry

The mass spectrum of SB3NO (**Figure 5**) showed a low-intensity parent peak at m/z 382 (3%), corresponding to its molecular mass of 381 g/mol. The molecular ion peak (M^+) undergoes fragmentation, as presented in **Figure 6**. Initially, the fragments at m/z 207 (21%) and m/z 171 (16%) were formed, likely due to the homolytic cleavage of the hydrazinic nitrogen bond. Following that, the loss of thiocyanic acid HSCN (56 g/mol) from the peak at m/z 171 yielded the benzylthiyl radical at m/z 121 (50%). Then, the benzylthiyl radical likely underwent cleavage of the C–S bond (32 g/mol), and the rearrangement of the benzyl group led to the formation of tropylium ion (m/z 91). The tropylium ion ($C_7H_7^+$) at m/z 91 was observed as the base peak. Lastly, the final fragment at m/z 54 represented a further cleavage of the tropylium ion ($C_7H_7^+$), resulting in the cyclobutadienyl cation (**$C_4H_3^+$**), formed through sequential cleavage of carbon atoms [18]. In conclusion, mass spectrometry data of SB3NO showed the same compound observed in the solid state with the observed molecular ion peak at m/z 382 along with the fragmentation peaks at m/z 207, 171, 121, 91, and 54.

Molar conductivity, magnetic moment and electronic spectral data

The molar conductance values of all the metal complexes (**Table 4**) were found to be in the range of 12.29 to 19.83 ohm^{-1} mol^{-1} cm^2, indicating their non-electrolytic nature. The conductivity values for a non-electrolyte in a DMSO solution are typically less than 50 ohm^{-1} mol^{-1} cm^2, which is consistent with past literature [19]. This suggests that SB3NO is directly bound to the metal ions without dissociating in the solution.

Table 3. ^{1}H-NMR and ^{13}C-NMR spectral data for SB3NO

Compound	^{1}H-NMR, δ (ppm)				^{13}C-NMR, δ (ppm)				
	N-H (thione)	S-CH_2	S-H (thiol)	Aromatic proton	C=S (thione)	C=O	C=N (thiol)	S-CH_2	Aromatic carbon
SB3NO	d, H (4.37, 4.39), d, H (4.49, 4.51)	s, 2H (4.59)	s, H (4.09)	m, (8.45-7.22, J = 7.0 Hz, 8H)	200.17	165.81	154.66	36.99 (thione), 37.53 (thiol)	147.67-126.37

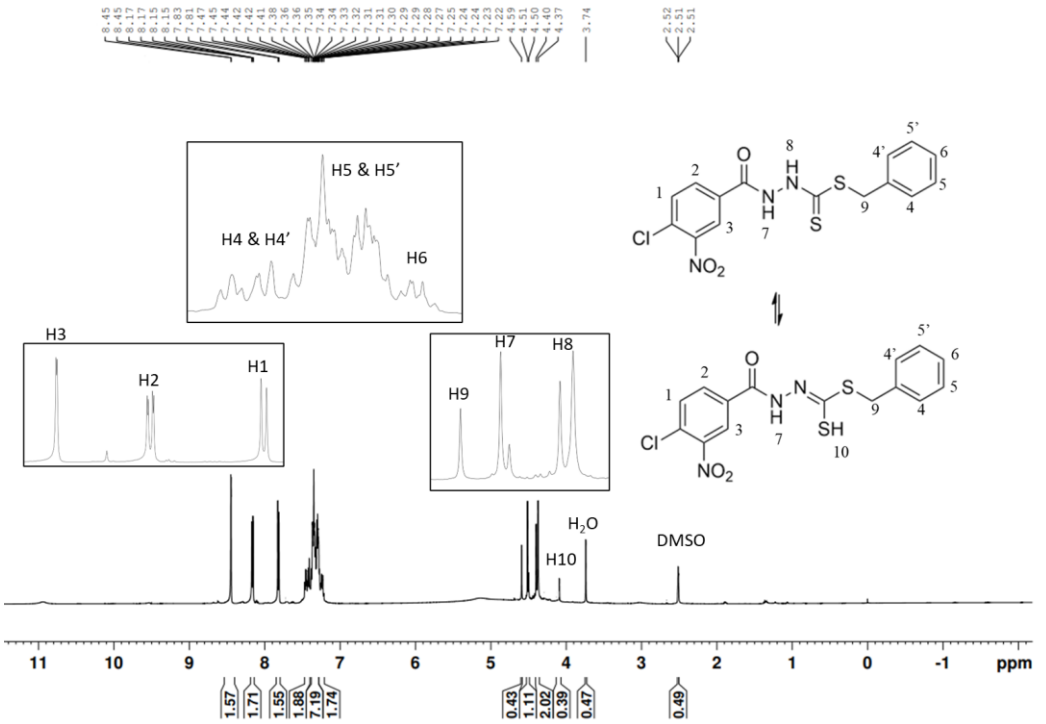

(a)

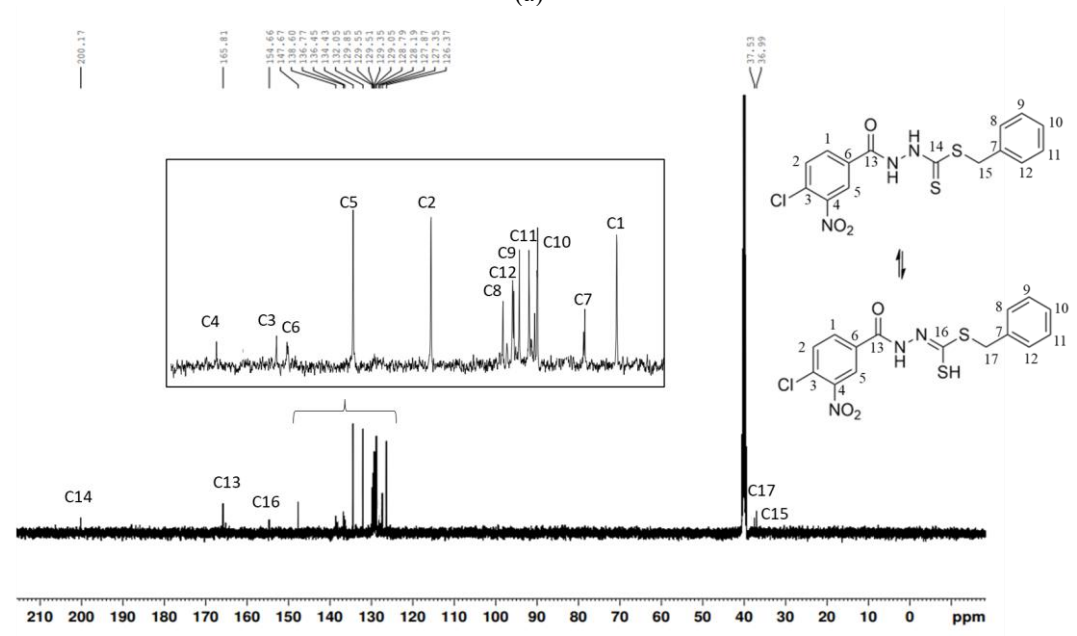

(b)

Figure 4. ^{1}H-NMR and ^{13}C-NMR spectral data for SB3NO.

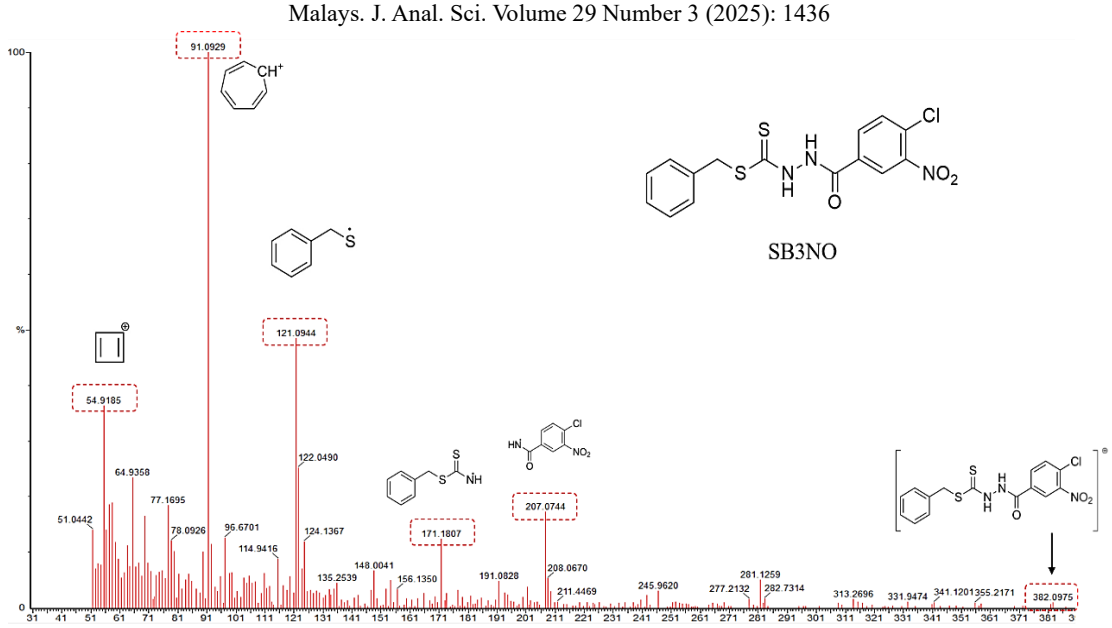

Figure 5. Mass spectrum of SB3NO

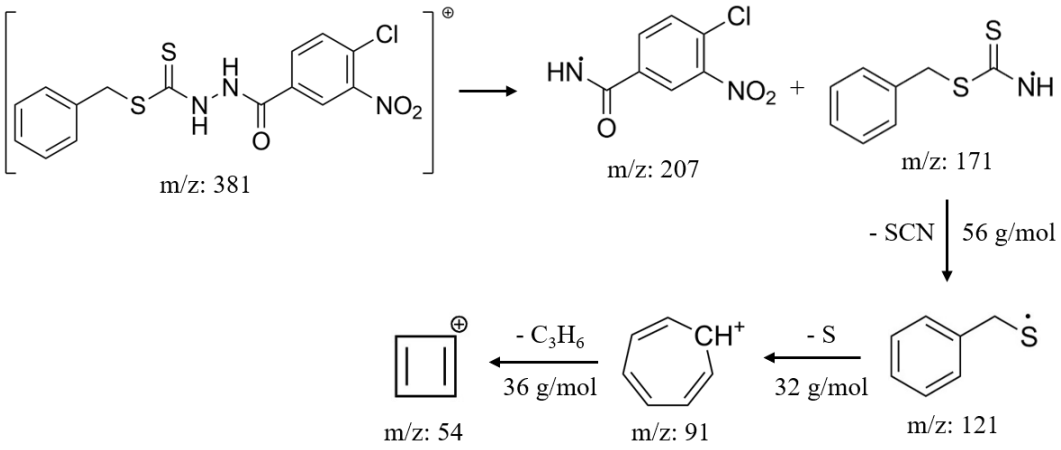

Figure 6. Fragmentation ions of SB3NO

The magnetic moments in **Table 5** showed that among all the synthesised complexes, only the Zn (II) complex exhibited a zero value for the magnetic moment, indicating its diamagnetic properties. Thus, the diamagnetism of $Zn(SB3NO)_2$ undergoes sp^3 hybridization to form a tetrahedral. $Cu(SB3NO)_2$ adopts a square planar geometry with a magnetic moment of 1.536 B.M, which agrees with previous literature [12]. Additionally, $Co(SB3NO)_2$ displayed a magnetic moment of 4.564 B.M, suggesting that it adopts a tetrahedral structure [11]. Lastly, the paramagnetic $Ni(SB3NO)_2$ complex presented a magnetic moment of 3.874 B.M, aligning with a tetrahedral configuration. Thus, based on magnetic susceptibility analysis, all metal complexes from SB3NO are confirmed to have a tetrahedral geometry except for $Cu(SB3NO)_2$, which exhibits a square planar geometry.

On the other hand, the electronic spectra data of SB3NO and its metal complexes are presented in **Table 5**. SB3NO exhibited two highly intense bands at 258 and 302 nm, corresponding to the π→π* transitions and n→π* transitions of the benzene rings, respectively [20]. Upon complexation, the π→π* transitions showed minimal shifts in the absorbance bands at 261-274 nm. All metal complexes, except $Co(SB3NO)_2$, exhibited a bathochromic shift of the n→π* transitions in the region 319-338 nm. The position of the absorption bands is significantly influenced by the characteristics of the metal ions. Chen et al. (2007) found that bathochromic shifts are often impacted by the electronegativity of the metal ions coordinating with the same ligand in the formation of metal complexes [21].

Additionally, a significant band around 354-389 nm was attributed to the ligand to metal charge transfer (LMCT) transition and was observed in all the metal complexes, except $Cu(SB3NO)_2$ [22]. Furthermore, only the Ni(II) complex displayed a low-intensity band at 500-800 nm, corresponding to the forbidden *d→d* transition [6]. According to El-Samanody et al., $Ni(SB3NO)_2$ exhibited two *d→d* transitions at approximately 606 and 456 nm, assigned to $^3A_{2g}\rightarrow{}^3T_{2g}(F)$, supporting a tetrahedral geometry [23]. Overall, the electronic spectra data supported the proposed geometries as deduced from the magnetic moment of the metal complexes.

Thermogravimetric analysis

Thermal stability and decomposition data of all the compounds are listed in **Table 5**. Generally, the TGA curve of SB3NO and metal complexes showed three and four thermal decomposition stages, respectively (**Figure 7**). SB3NO began to decompose at 130°C, continuing until 226°C with a mass loss of 26.04% (Calculated: 23.88%) due to the loss of the benzyl group from SBDTC [24]. Then, a weight loss of 47.70% (Calculated: 48.03%) was observed between 226°C and 295°C, attributable to the loss of the 3-nitro-4-chlorobenzoyl group. The decomposition of the hydrazine group occurred above 295°C, resulting in a mass loss of 8.034% (Calculated: 7.87%). Lastly, the remaining residue comprises the S-C=S, which accounted for a loss of 20.47% (Calculated: 19.94%) [25].

The metal complexes from SB3NO, on the other hand, demonstrated a complicated decomposition process. Notably, only $Cu(SB3NO)_2$ exhibited significant weight loss, exceeding half of its mass (as illustrated in **Figure 7**), implying the necessity for higher heating temperatures for other metal complexes. The decomposition of $Cu(SB3NO)_2$, began in the range of 127-372 ºC, resulting in a mass loss of 52.50% (Calculated 59.95%), indicative of the dissociation of all aromatic rings from SB3NO along with the dissociation of the chloro and nitro groups [26]. Next, the hydrazine group was removed in the subsequent stage around 372-564 ºC, leading to a mass loss of 13.72% (Calculated 10.19%). A minor weight loss, observed at 564-735 ºC, accounting for 3.55% (Calculated 2.91%), corresponds to carbon removal. A negligible weight loss of 1.15% was observed at 735-800 ºC was disregarded. Consequently, the residual mass of 26.61% (Calculated: 23.17%) comprises copper oxide and the S-C=S group [27]. $Zn(SB3NO)_2$ only decomposed 38.442 % of its mass, with the majority loss occurring in the first stage at 132-298 with a mass loss of 22.39% (Calc. 22.08%), which is assigned to the benzyl group from SBDTC. Then, the nitro group was removed in the second stage around 298-467 ºC, resulting in a mass loss of 10.17% (Calculated 11.15%). The third stage involved the decomposition of the chloride group at 467-615 ºC, resulting in a mass loss of 5.60% (Calculated 8.23%). Negligible mass loss observed in the final stage was disregarded, leaving the remaining products, including zinc oxide, dithiocarbazate moiety, and aromatic ring from the 3-nitro-4-chlorobenzoyl group with a mass of 61.16% (Calculated 61.56%).

$Co(SB3NO)_2$ and Ni(SB3NO) exhibited similar decomposition patterns. At the initial stage, both compounds underwent decomposition of the benzyl group from SBDTC around 136-323 ºC and 110-273 ºC, resulting in mass loss of 22.71% (Calculated 22.22%) and 20.09% (Calculated 22.24%), respectively. Subsequently, the nitro and chloro group was dissociated from $Co(SB3NO)_2$ at 323-420 ºC and 420-518 ºC, resulting in mass loss of 10.17% (Calculated 11.15%) and 5.60% (Calculated 8.17%), respectively. However, both fragments decomposed at the same stage in $Ni(SB3NO)_2$ around 273-426 ºC, resulting in a mass loss of 17.77% (Calculated 16.85%). For $Co(SB3NO)_2$, a minor loss observed at 518-800 ºC, accounting for 7.45% (Calculated 7.27%), corresponds to the removal of the hydrazine group. Meanwhile, $Ni(SB3NO)_2$ exhibited negligible losses in both final stages at 426-733 ºC and 733-800 ºC, with mass losses of 2.95% and 1.547%, respectively. As a result, the remaining compounds from both $Co(SB3NO)_2$ and $Ni(SB3NO)_2$ were found to be metal oxide, dithiocarbazate moiety, and the aromatic ring of the masses of 52.38% (Calculated 54.07%) and 60.88% (Calculated 57.643%), respectively.

Overall, metal complexes showed more decomposing stages and higher decomposing temperatures compared to SB3NO. Thus, it is suggested that the metal complexes are more thermally stable than SB3NO due to the presence of metal ions. The remaining residue, especially in metal complexes, was stabilised by strong coordination bonds between donor atoms such as nitrogen, oxygen, and sulfur with metal ions, creating a stable metal complex [24]. Thus, breaking these bonds required temperatures exceeding 1000°C due to their high bond dissociation energies.

Table 4. Electronic spectra, magnetic moment and molar conductivity data of SB3NO and its metal complexes

Compound	λ_{max}, nm (log e, cm^{-1} mol^{-1} L)	μ_{eff} (B.M.)	Molar conductivity (ohm^{-1} mol^{-1} cm^2)
SB3NO	258 (3.963), 302 (3.684)	-	-
$Cu(SB3NO)_2$	263 (3.93), 319 (3.795)	1.536	15.51
$Zn(SB3NO)_2$	263 (4.070), 338 (3.865), 354 (3.800)	Diamagnetic	19.83
$Co(SB3NO)_2$	261 (3.943), 301 (3.945), 389 (3.588)	4.564	18.5
$Ni(SB3NO)_2$	274 (3.851), 326 (3.828), 383 (3.527), 456 (3.136), 606 (2.397)	3.874	12.29

Table 5. Thermal properties of SB3NO and its metal complexes

Compound	Total Weight Loss (%)	Decompose Temperature (°c)	Percentage Loss (%)
SB3NO	81.774	130-226	26.04
		226-295	47.70
		295-500	8.034
$Cu(SB3NO)_2$	70.921	127-372	52.50
		372-564	13.72
		564-735	3.55
		735-800	1.15
$Zn(SB3NO)_2$	38.442	132-298	22.39
		298-467	10.17
		467-615	5.60
		615-800	0.28
$Co(SB3NO)_2$	45.93	136-323	22.71
		323-420	10.17
		420-518	5.60
		518-800	7.45
$Ni(SB3NO)_2$	42.357	110-273	20.09
		273-426	17.77
		426-733	2.95
		733-800	1.547

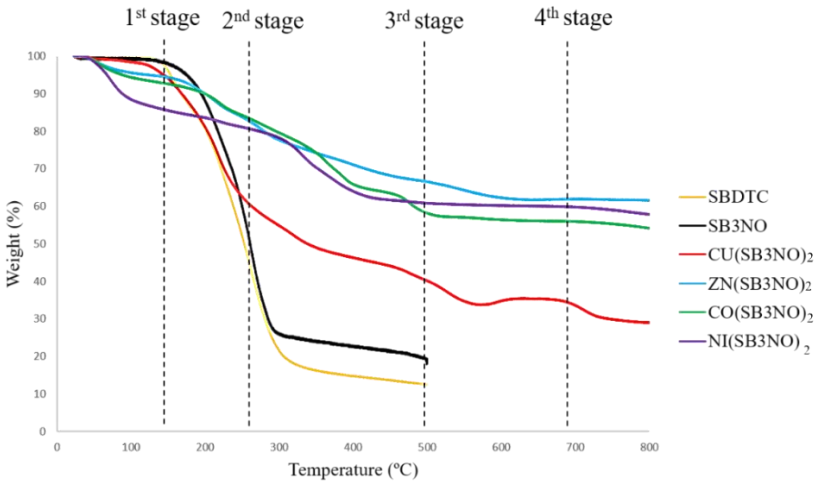

Figure 7. Thermal decomposition of SB3NO and its metal complexes

Antimicrobial assay

Table 6 presents the minimal inhibitory concentration (MIC) values for SB3NO and its metal complexes. For *S. aureus* (ATCC 25923), a gram-positive bacterium, SB3NO showed a high MIC of 3500 µg/mL. Upon complexation with metal ions, there was a notable improvement in their antibacterial properties. $Cu(SB3NO)_2$, displayed a

reduced MIC value of 1750 µg/mL, while the $Zn(SB3NO)_2$, $Co(SB3NO)_2$, and $Ni(SB3NO)_2$ exhibited a MIC value of 875 µg/mL. Similarly, SB3NO, $Cu(SB3NO)_2$, and $Ni(SB3NO)_2$, demonstrated an MIC of 1750 µg/mL against *B. cereus* (ATCC 11778), whereas the zinc and cobalt complexes effectively displayed a reduced MIC of 875 µg/mL. This trend highlights that the zinc and cobalt complexes significantly enhance the antibacterial effects against gram-positive bacteria.

On the other hand, SB3NO exhibited a MIC of 1750 µg/mL against both gram-negative bacteria, *E. coli* (ATCC 25922) and *P. aeruginosa* (ATCC 27853). Upon complexation, the copper, cobalt, and nickel complexes did not show any enhancement, maintaining the same MIC values. However, the zinc complex demonstrated superior efficacy, lowering the MIC to 875 µg/mL and 437 µg/mL against *E. coli* (ATCC 25922) and *P. aeruginosa* (ATCC 27853), respectively. Thus, it showed that zinc complexation plays a particularly crucial role in enhancing the activity of SB3NO against gram-negative bacteria.

However, when compared to the positive control in these studies, gentamicin exhibits the strongest antibacterial activity, with MIC values of 32 µg/mL for *S. aureus*, 16 µg/mL for *B. cereus* and *E. coli*, and 8 µg/mL for *P. aeruginosa*. Moreover, ampicillin also demonstrates superior activity, with MIC values of 113 µg/mL for *S. aureus, B. cereus*, and *P. aeruginosa*, and 226 µg/mL for *E. coli*. None of the synthesized compounds surpass or match the antibacterial activity of gentamicin or ampicillin. This suggests that further structural modifications may be necessary to enhance their antibacterial efficacy.

The data also indicates that gram-positive bacteria are more susceptible to inhibition by SB3NO and its metal complexes compared to gram-negative bacteria, except for $Zn(SB3NO)_2$, which selectively inhibits *P. aeruginosa* (ATCC 27853). The increased susceptibility to gram-positive bacteria is primarily attributed to the structural differences. Gram-negative bacteria possess an additional, highly impermeable outer membrane that acts as a formidable barrier against antimicrobial agents, making them inherently more resistant [28]. In contrast, gram-positive bacteria lack this outer layer, rendering them more accessible to antibacterial compounds [29].

Furthermore, while SB3NO alone showed moderate antimicrobial activity, the formation of metal complexes, particularly with $Zn(SB3NO)_2$ was the most promising metal complex. The enhanced antibacterial efficacy of the metal complexes is attributed to significant physicochemical changes during chelation, which reduce polarity and increase lipophilicity in aqueous solutions [30]. This improved interaction with biological membranes facilitates better penetration and antimicrobial effectiveness.

In conclusion, even though the MIC values of SB3NO and their metal complexes were higher than those of commercial antibiotics, their potential remains significant. The observed biological activity suggests these compounds could be further optimised to enhance their antimicrobial properties. Additionally, the ability of certain metal complexes such as $Zn(SB3NO)_2$ to inhibit bacteria better than free ligands alone presents a promising path for the development of new and potent metal-based antimicrobial agents.

Table 6. Antimicrobial activity of SB3NO and its metal complexes

Compound	**MIC (µg/mL)**			
	Gram-Positive Bacteria		**Gram-Negative Bacteria**	
	***S. aureus* (ATCC 25923)**	***B. cereus* (ATCC 11778)**	***E. coli* (ATCC 25922)**	***P. aeruginosa* (ATCC 27853)**
SBDTC	875	437	437	875
SB3NO	3500	1750	1750	1750
$Cu(SB3NO)_2$	1750	1750	1750	1750
$Zn(SB3NO)_2$	875	875	875	437
$Co(SB3NO)_2$	875	875	1750	1750
$Ni(SB3NO)_2$	875	1750	1750	1750
Gentamycine	32	16	16	8
Ampiciline	113	113	226	113

Conclusion

New dithiocarbazate derivatives, *S*-benzyl-4-chloro-3-nitrodithiocarbazate (SB3NO), derived from the reaction of 4-chloro-3-nitrobenzyl chloride with S-benzyldithiocarbazate (SBDTC) acts as a uninegative bidentate ligand with its OS donor set to form bis chelated Cu(II), Zn(II), Co(II) and Ni(II) complexes. The Cu(II) complexes have a square planar geometry, while the Zn(II), Co(II) and Ni(II) complexes are tetrahedral. In solid, SB3NO predominantly exists as the thione tautomeric form, while in liquid, it is present as a mixture of thione-thiol tautomeric forms in the ratio of 2:1, as evidenced by the FTIR and NMR analyses. Antimicrobial activity studies demonstrated that metal complexes enhanced the inhibition activity of SB3NO. Among them, $Zn(SB3NO)_2$ showed the most promising antibacterial potential by inhibiting *P. aeruginosa* (ATCC 27853), with an MIC of 437 µg/mL. Overall, the findings suggest that metal complexes not only enhance antimicrobial efficacy but also serve as a promising strategy for developing novel antibacterial agents, providing a potential alternative to conventional antibiotics.

Acknowledgement

The authors thank the Department of Chemistry, Kulliyyah of Science, International Islamic University Malaysia Kuantan, for the provision of laboratory facilities. An appreciation was also given to Associate Professor Dr. Nadiah Halim from the University of Malaya for her assistance in the measurement of the magnetic susceptibility values.

References

1. Alexander, J. W. (2009). History of the Medical Use of Silver. *Journal of Surgical Infection*, 10 (3): 289-292.
2. Beceiro, A., Tomás, M., and Bou, G. (2013). Antimicrobial resistance and virulence: A successful or deleterious association in the bacterial world. *Clinical Microbiology Reviews*, 26: 185-230.
3. Pachori, P., Gothalwal, R., and Gandhi, P. (2019). The emergence of antibiotic resistance Pseudomonas aeruginosa in intensive care unit; a critical review. *Genes & Diseases*, 6: 109-119.
4. Gasser, G. (2015). Metal complexes and medicine: A successful combination. *Chimia*, 69: 442-446.
5. Huh, A. J., and Kwon, Y. J. (2011). "Nanoantibiotics": A new paradigm for treating infectious diseases using nanomaterials in the antibiotics resistant era. *Journal of Controlled Release*, 156: 128-145.
6. Bhat, R. A., Singh, K., Kumar, D., Kumar, A., and Mishra, P. (2022). Antimicrobial studies of the Zn(II) complex of S-benzyl-β-(N-2-methyl-3-phenylallylidene) dithiocarbazate. *Journal of Coordination Chemistry*, 75: 1050-1062.
7. Sohtun, W. P., Kathiravan, A., Asha Jhonsi, M., Aashique, M., Bera, S., and Velusamy, M. (2022). Synthesis, crystal structure, BSA binding and antibacterial studies of Ni(II) complexes derived from dithiocarbazate-based ligands. *Inorganica Chimica Acta*, 536: 120888.
8. Kargar, H., Ashfaq, M., Fallah-Mehrjardi, M., Behjatmanesh-Ardakani, R., Munawar, K. S., and Tahir, M. N. (2022). Unsymmetrical Ni(II) Schiff base complex: Synthesis, spectral characterization, crystal structure analysis, Hirshfeld surface investigation, theoretical studies, and antibacterial activity. *Journal of Molecular Structure*, 1265: 133381.
9. Rosnizam, A. N., Hamali, M. A., Low, A. L. M., Youssef, H. M., Bahron, H., and Tajuddin, A. M. (2022). Palladium (II) complexes bearing N, O-bidentate Schiff base ligands: Experimental, in-silico, antibacterial, and catalytic properties. *Journal of Molecular Structure*, 1260: 132821.
10. Ali, M. A., and Bose, R. (1977). Metal complexes of Schiff bases are formed by condensation of 2-methoxybenzaldehyde and 2-hydroxybenzal dehyde with S-benzyldithiocarbazate. *Journal of Inorganic and Nuclear Chemistry*, 39: 265-269.
11. How, F. N. F., Crouse, K. A., Tahir, M. I. M., Tarafder, M. T. H., and Cowley, A. R. (2008). Synthesis, characterization and biological studies of S-benzyl-β-N-(benzoyl) dithiocarbazate and its metal complexes. *Polyhedron*, 27: 3325-3329.
12. Break, M. K. Bin, Tahir, M. I. M., Crouse, K. A., and Khoo, T. J. (2013). Synthesis, characterisation, and bioactivity of Schiff bases and their Cd^{2+}, Zn^{2+}, Cu^{2+}, and Ni^{2+} complexes derived from chloroacetophenone isomers with S-benzyldithiocarbazate and the X-ray crystal structure of S-benzyl-β-N-(4-chlorophenyl) methylenedithiocarbazate. *Bioinorganic Chemistry and Applications*, 1: 362513.
13. Malmberg, C., Yuen, P., Spaak, J., Cars, O., Tängdén, T., and Lagerbäck, P. (2016). A novel microfluidic assay for rapid phenotypic antibiotic susceptibility testing of bacteria detected in clinical blood cultures. *Plos One*, 11: 167356.
14. Gwaram, N. S., Ali, H. M., Khaledi, H., Abdulla, M. A., Hadi, H. A., Lin, T. K., Ching, C. L., and Ooi, C. L. (2012). Antibacterial evaluation of some Schiff bases derived from 2-acetylpyridine and their metal complexes. *Molecules*, 17: 5952-5971.
15. T. W. Graham Solomons Craig B. Fryhle, and Snyder, S. A. (2016). *Organic Chemistry*: 1124

16. Tarafder, M. T. H., Ali, M. A., Wee, D. J., Azahari, K., Silong, S., and Crouse, K. A. (2000). Complexes of a tridentate ONS Schiff base. Synthesis and biological properties. *Transition Metal Chemistry*, 25(4): 456-460.
17. Akbar Ali, M., and Livingstone, S. E. (1974). Metal complexes of sulphur-nitrogen chelating agents. *Coordination Chemistry Reviews*, 13: 101-132.
18. Cohen, L., Go, E. P., and Siuzdak, G. (2007). Small-molecule desorption/ionization mass analysis. *MALDI MS*: 299-337.
19. Ali, I., Wani, W. A., and Saleem, K. (2013). Empirical formulae to molecular structures of metal complexes by molar conductance. *Synthesis and Reactivity in Inorganic, Metal-Organic and Nano-Metal Chemistry*, 43: 1162-1170.
20. Guo, L., Wu, S., Zeng, F., and Zhao, J. (2006). Synthesis and fluorescence property of terbium complex with the novel Schiff-base macromolecular ligand. *European Polymer Journal*, 42: 1670-1675.
21. Chen, Z., Wu, Y., Gu, D., and Gan, F. (2007). Spectroscopic, and thermal studies of some new binuclear transition metal(II) complexes with hydrazone ligands containing acetoacetanilide and isoxazole. *Spectrochimica Acta Part A: Molecular and Biomolecular Spectroscopy*, 68: 918-926.
22. Mahmoud, W. A., Hassan, Z., and Russel W. (2020). Synthesis and spectral analysis of some metal complexes with mixed Schiff base ligands 1-[2-(2-hydroxybenzylideneamino)ethyl]pyrrolidine-2,5-dione (HL1) and (2-hydroxybenzalidine)glycine (HL2). *Journal of Physics: Conference Series*, 1660: 12027.
23. El-Samanody, E. S. A., AbouEl-Enein, S. A., and Emara, E. M. (2018). Molecular modelling, spectral investigation and thermal studies of the new asymmetric Schiff base ligand; (E)-N'-(1-(4-((E)-2-hydroxybenzylideneamino)phenyl)ethylidene)morpholine-4-carbothiohydrazide and its metal complexes: Evaluation of their antibacterial and anti-molluscicidal activity. *Applied Organometallic Chemistry*, 32: 4262.
24. Thermogravimetric analysis. (2018). A practical guide to microstructural analysis of cementitious materials: pp. 196-231.
25. PerkinElmer. (2010). A beginner's guide to thermogravimetric analysis: pp. 209-287.
26. Singh, M., Aggarwal, V., Singh, U. P., and Singh, N. K. (2009). Synthesis, characterization and spectroscopic studies of a new ligand [N′-(2-methoxybenzoyl)hydrazinecarbodithioate] ethyl ester and its Mn(II) and Cd(II) complexes: X-ray structural study of Mn(II) complex. *Polyhedron*, 28: 107-112.
27. Yekke-Ghasemi, Z., Ramezani, M., Mague, J. T., and Takjoo, R. (2020). Synthesis, characterization and bioactivity studies of new dithiocarbazate complexes. *New Journal of Chemistry*, 44: 8878-8889.
28. Bos, M. P., and Tommassen, J. (2004). Biogenesis of the Gram-negative bacterial outer membrane. *Current Opinion in Microbiology*, *7*: 610–616.
29. Malanovic, N., and Lohner, K. (2016). Gram-positive bacterial cell envelopes: The impact on the activity of antimicrobial peptides. *Biochimica et Biophysica Acta (BBA)-Biomembranes,* 1858: 936-946.
30. Bhowmick, A. C., Bhowmick, A. C., Dev Nath, B., and Moim, M. I. (2019). Coordination complexes of transition metals and Schiff base with potent medicinal activity. *American Journal of Chemistry*, 4: 109-114.